Mansoura University
Faculty of Engineering
Mansoura Engineering Journal

Approximate static analysis of circular convex cable roof beams in the existence of central and edge rings

التحليل الإستاتيكي التقريبي لكمرات الأسقف الدائرية المحدبة ذات الكابلات في وجود حلقات مركزية وحافة

Y. E. Aggag, M. Naguib, S. El Bagalaty, and A. M. Abbas

KEYWORDS:

Tension structures, cables , circular roofs, convex beams, preliminary analysis

الهدف الرئيسي من هذا العمل هو دراسة العوامل التي تؤثر على السلوك الاستاتيكي لكمرات الأسقف المحدبة ذات الكابلات ذات حلقات مركزية وحافة، مع الأخذ في الاعتبار السلوك الغير خطي لاقتراح نهج مناسب للاستخدام في الحسابات الابتدائية والتصميم. في مثل هذه الأسقف، عادة ما يتم تعليق الكابلات شعاعيا حيث تعلق في محيط السقف إلى حلقة ضغط ذات تشوه مرن وفي المركز إلى حلقات شد معدنية. وقد تم تحليل منشأ له خصائص هندسية وميكانيكية محددة إستنادا على طريقة تصغير طاقة الوضع باستخدام طريقة المنحدرات المتبادلة لإنتاج جداول، منحنيات لا بعديه وعلاقات للتحويل تستخدم في التصميم الابتدائي. طريقة التصميم الابتدائية المقترحة قابلة للتطبيق على أي منشأ ذو خصائص مماثلة ويمكن استخدامها لحساب التشكلات القصوى للسقف، الشد الأقصى في الكابلات المعلقة، الشد الأدنى في الكابلات المقوسة والقوي العمودية القصوى في الحلقات. ويلاحظ أن الطريقة أظهرت نتائج جيدة مقارنة مع طرق التحليل الدقيقة التي تستخدمها عادة برامج التحليل الإنشائي التجارية وأيضا يمكن تطويرها بسهولة لاستخدامها في كمرات الأسقف المقعرة والمحدبة-المقعرة ذات الكابلات ذو مساقط مختلفة.

***Abstract*— The key objective of the present work is to study the parameters affecting the static behavior of convex cable roof beams with central and edge rings, taking into consideration the nonlinear behavior to propose an appropriate approach for their preliminary calculations and design aspects. In such roofs, the cables are commonly suspended radially and attached at the perimeter of the roof to an elastically deformable compression edge ring and at the center to tension steel rings. A structure with a specific geometrical and mechanical properties has been analyzed based upon the minimization of the total potential energy by the conjugate gradient method to produce nondimensional curves, tables, and transformation expressions used for the preliminary design. The suggested preliminary approach is applicable for any structure with similar characteristics and can be used to determine the maximum roof deformations, maximum tensions of the sagging cables, minimum tensions of the hogging cables, and the maximum normal forces in the rings. It is noted that the method show good results compared to the exact analysis methods commonly used by commercial programs in structural analysis, and can be readily developed to be used for concave, convex-concave cable beam roofs with different plans of view.**

Received:: 31 May, 2018 - Accepted: 4 July, 2018

Y. E. Aggag, Emeritus Professor in Department of Structural Engineering, Faculty of Engineering, Mansoura University (e-mail: youssefagag@gmail.com).

M. Naguib, Emeritus Professor in Department of Structural Engineering, Faculty of Engineering, Mansoura University (e-mail: naguib2005@yahoo.com).

S. El Bagalaty, Assistant Professor in Department of Structural Engineering, Faculty of Engineering, Mansoura University (e-mail: dr.salah.bagalaty@gmail.com).

A. M. Abbas, Demonstrator in Department of Structural Engineering, Faculty of Engineering, Mansoura University (e-mail: a_m_abbas@ mans.edu.eg).

I. INTRODUCTION

In recent decades, cable structures have been considered an economical alternative over traditional portal and conventional structural systems for their mechanical properties and load carrying efficiency. Cable elements work only in pure axial tension and can carry large loads much more than their own weight. Therefore, their

spacing can be greatly increased to cover long spans without causing stability issues [1]. Also, from the architectural point of view, their lightness offer an infinite number of possibilities for shaping unique and elegant three dimensional roofing forms with rectangular, rhomboid, circular or elliptical plans [2].

Disadvantages also appear as the high geometric nonlinearity of cables is always a challenge to the stability of structures. When a cable subjected to variable loading conditions, it undergoes large movements that increase the difficulty of the analysis and design procedure [3]. Therefore the principle of superposition does not acceptable for such systems, and it is strongly recommended to take the effects of cables flexibility and their large deformations into concern when establishing equilibrium equations [4].

Thus, preliminary techniques are valuable in order to reduce the computational effort exerted in estimation of cable sizes, their pretention forces, initial costs and materials required [5]. Many analytical researches supposed infinitely rigid supports for cable edges, and ignore deformations and flexibility of the supporting structures, i.e., edge rings, stays, and columns. The first effort adopts the former principle for preliminary analysis of cable networks has been carried out by Gero [6]. The method is based on preforming geometrically nonlinear analyses to produce scaling relationships and charts. These relationships are used for transformation of a much larger analysis problem called the prototype to a smaller network denoted as the model. The prototype and the model, should have similar geometries, so that their corresponding characteristics also be similar.

However, studies show that the deformability of the boundary at joints of cable attachments, results a loss in the tension of the cables and a variation in the net deflections [7]. Thus the static and dynamic characteristics of a cable structure will vary depending upon the stiffness of the supporting system. The latter in turn is a function of the element geometry and type of the material used. Useful approximate procedures for certain cases of cable systems have been developed by Talvik [8], Majowiecki, and Zoulas [9]. Also, Szabó et. al. [10] supposed another preliminary method for analysis of cable networks with elliptical plan view, where cable ends are attached to an edge beam. Isabella Vassilopoulou and Charis J. Gantes [11], have been extending the transformation relations that established by Gero [6] to be applicable for circular cable networks supported by an elastically deformable ring beam, taking into consideration the ring stiffness and the curvature of the cables, i.e. sag and rise to span ratios.

The main objective of the present work is to study the static behavior of circular convex cable roof beams, through geometrically nonlinear analyses. Tables and graphs illustrate the response are given in nondimensional form, and represent the guidelines to derive transformation relations used for the preliminary design of such roofs. The analysis is carried out by a FORTRAN computer program based on the minimization of the total potential energy (T.P.E.) of the structure using the conjugate gradient method [12]. Selected examples have been resolved to verify and confirm the results obtained using SAP2000 [13].

II. MODEL CHARACTERISTICS AND PARAMETRIC STUDIES

In case of roofs with circular plans, cable beams can be distributed radially and attached at the center to a small steel tension ring and at the perimeter to a compression edge ring commonly made of prestressed concrete with a square or a rectangular cross sections, as shown in Figs. 1(a), (b), (c), and (d) [14]. A study of a convex cable system of the type shown in Fig. 1(b) is presented to determine its static response for variation in particular significant parameters now follows.

These parameters include the cable sizes, pretension forces, and their curvatures. Also the effect of the rigidity and deformability of flexural elements on the behavior are included. The study is carried out considering one variable parameter, and others are constant in each case. The net shown in Fig. 2, with various sections of structural elements shown in Fig. 3, is proposed for the analysis.

To simplify notations and in order to avoid misunderstanding, in case of equal properties for both the sagging and the hogging cables, each of the extensional rigidity, the pretension force, and the cables curvature may be termed as *EA*, *H*, and *f/L* respectively.

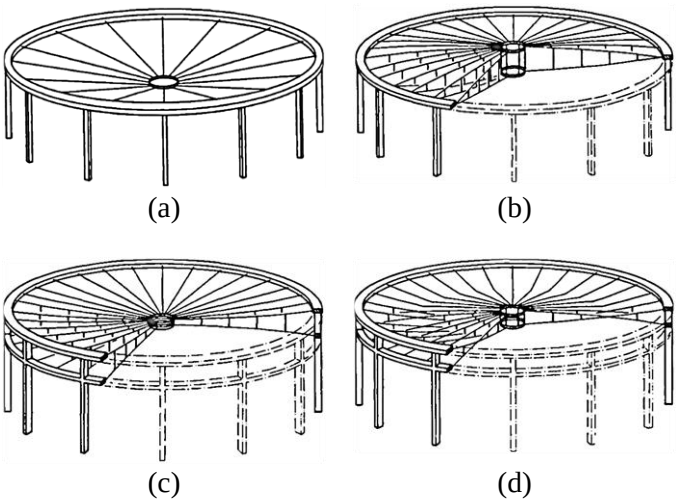

Fig. 1. Circular cable roofs with cables suspended in radial planes between central tension ring/s and outer edge ring/s: (a) Simply suspended cable roof; (b) Convex cable beam structure; (c) Concave cable beam structure; (d) Convex-concave cable beam structure.

The static analysis is carried out for a cable net having a span of 80m, sag to span ratio 4%, and rise to span ratio 4%. The net consists of 42 pairs of convex cable beams distributed radially between two steel central rings and a single R.C. edge ring, where the diameters ratio for central to edge rings is considered as 8.0%. The cable beam consists of a dual-cable counter stressed system with properties shown in Table. 1. Both the lower sagging, and the top hogging cables have extensional rigidities of 297.7 MN, and the same pretension forces of 570 KN. While, the 12 struts are made of steel pipes

with extensional rigidity of 19.95 MN.

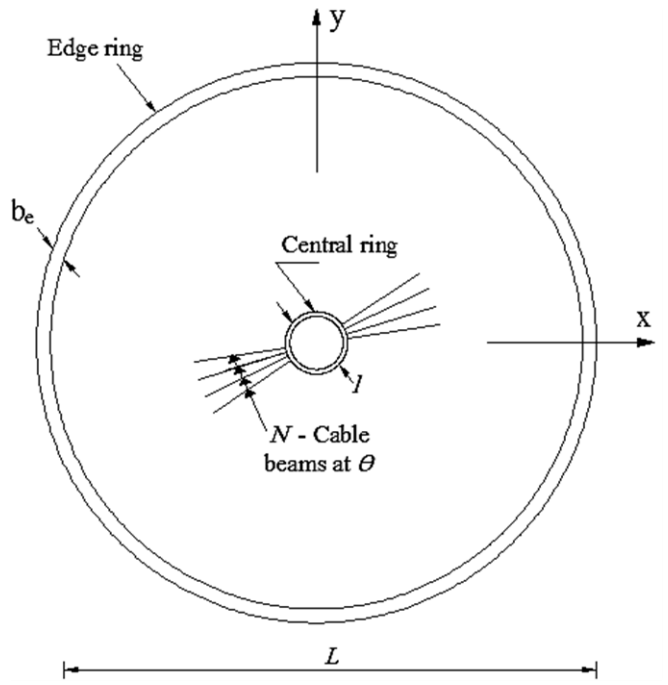

Fig. 2. Plan view of radial convex cable beam structure

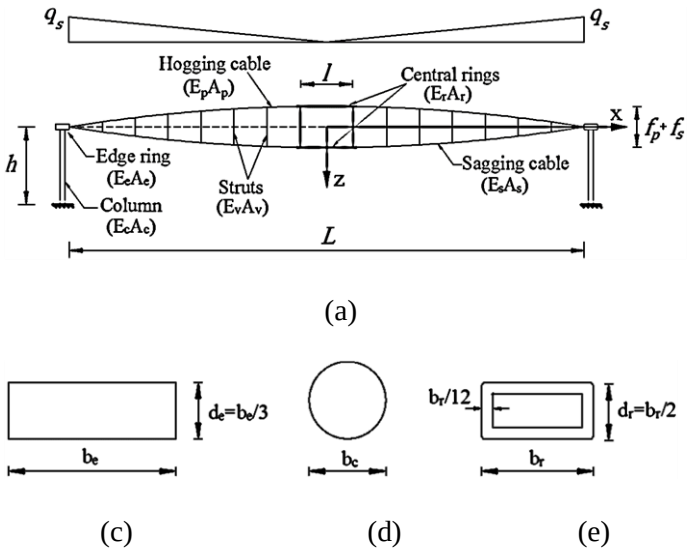

Fig. 3. Convex cable beam structure: (a) Cross section through the roof; (b) Cross section of the R.C. edge beam; (c) Cross section of the R.C. column; (d) Cross section of the steel central ring.

Table. 2 shows the characteristics of the flexural elements utilized in the analysis. The edge ring has a rectangular reinforced concrete section with extensional rigidity of 49980 MN. While, central rings have a rectangular hollow steel section with extensional rigidity 6699 MN. Each cable connection at the edge ring is supported vertically with reinforced concrete columns have circular sections with extensional rigidity of 17102 MN. All Columns have a mean height of 10 m and supposed to be fixed at base.

For circular roofs in which the cable beams radiate out from a centrally suspended tension ring, it is convenient to express the distributed load applied on each beam as a two symmetrically triangular distributed loads with a maximum intensity placed on the upper cable [15]. Uniformly distributed loads used are based on the following values:

- Dead load of the roof = 400 N/m^2 of projected area
- Live loads = 500 N/m^2 of projected area

For the purpose of analysis, the triangularly distributed loads are assumed to be applied as a system of equivalent concentrated forces equally spaced and applied on the joints of the hogging cable.

The obtained results are prepared in a nondimensional formulae for the maximum positive deflection of the net (w), maximum radial deformations of the edge ring (u_e), the minimum hogging cable tension (T_p), the maximum sagging cable tension (T_s), the upper central ring tension (P_p), the lower central ring tension (P_s), the edge ring compression (P_e), and the maximum bending moment at the level of fixed base (M_b).

TABLE 1
PROPERTIES OF CABLES UTILIZED IN THE PARAMETRIC STUDY

Cross sectional area , A (cm^2)	18
Modulus of elasticity, E (MPa)	165500
Pretension force, H (KN)	570
Weight per unit length, (N/m)	140.4

TABLE 2
PROPERTIES OF FLEXURAL ELEMENTS UTILIZED IN THE PARAMETRIC STUDY

Parameters	Edge ring	Column	Central rings
Cross sectional area , A (m^2)	1.47	0.503	0.0319
Modulus of elasticity, E (MPa)	34000	34000	210000
Moment of inertia, Ixx (m^4)	0.06	0.0201	1.29×10^{-4}
Moment of inertia, Iyy (m^4)	0.54	0.0201	4.33×10^{-4}
Moment of inertia, Izz (m^4)	0.19	0.0402	2.99×10^{-4}
Weight per unit length, (KN/m)	36.75	12.575	2.49

Many study parameters are considered as:

A. Effect of the curvature of cables and the load intensity on the response

In general, geometric nonlinearity is a principle feature of cable structures analyzing. It is affected by the stiffness of the structure which is a function of the pretension forces, curvature of the cables, and the stiffness of the supporting system [16]. Many researchers suggested that the satisfactory

stiffness of the cable net will be accomplished if the maximum sag of the sagging cable is within 4% and 6% of the span [17].

The beams are analyzed in order to provide insight into the behavior of the system due to the cables curvature under varying loading intensities from 150 N to 1150 N. Different cases of equal sag and rise to span ratios with f/L = 3%, 4%, 5%, and 6% are considered.

The deformed shape of the structure is sketched in Fig. 4. Also, values of maximum deflections of the net along z axes, maximum deformations of the edge ring, maximum and minimum cables tensions, and maximum normal forces of rings are plotted in Figs. 6 to 13.

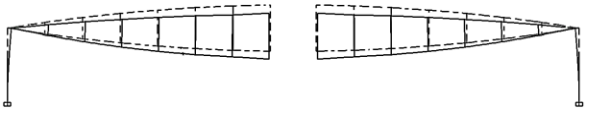

(a) Deformed shape due to pretension forces only

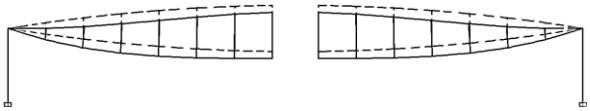

(b) Deformed shape due to the case of dead + live loads

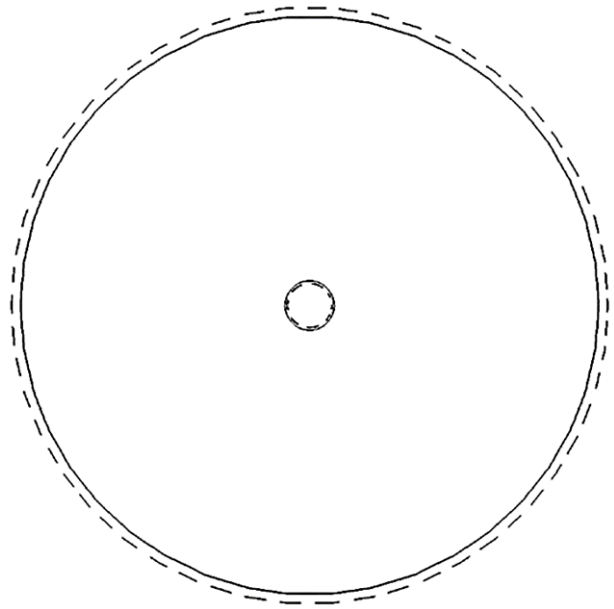

(c) Deformation of rings

Fig. 4. Illustrative sketches of the deformed structure

It is noted that:

1. The system becomes stiffer and responds in less nonlinear manner with increasing of the load intensity and sag/rise to span ratios.
2. The nonlinear response of the cables causes a nonlinear response of the rings.
3. Due to rising loading of the net, the tension change in the sagging cables is much larger than that in the hogging cables, therefore the sagging cables may be properly termed as the primary cables, whilst the hogging cables are called the secondary cables, Fig. 5(a).
4. The tension along a cable slightly increases towards the edge ring, such as the vertical component is increased to balance the increased shear force due to the existing loads, although its horizontal component remains constant.
5. The rate of change in the tensile force of the cables is small from segment to another. Thus, the design of tension for the whole cable can be adopted as the same value without any considerable loss in economy.
6. The principal mode of action of the edge ring is axial compression, while that for both central rings is direct axial tension, Fig. 5(b). Therefore, in the final deformed shape of the net, opposite joints of the edge ring are approaching each other, Fig. 4(c).
7. Increasing the sag/rise to span ratios cause a decrease of the maximum deflections of the net, the maximum tension of sagging cables, tensions of the lower central ring, and compressive force of the edge ring. While, tensions of the upper central ring and hogging cables are increased.

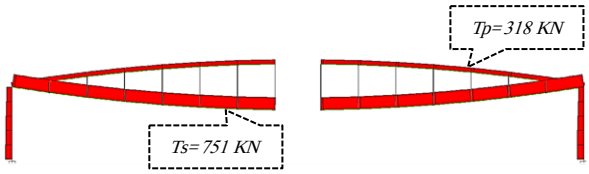

(a) Cable tensions and column compressions

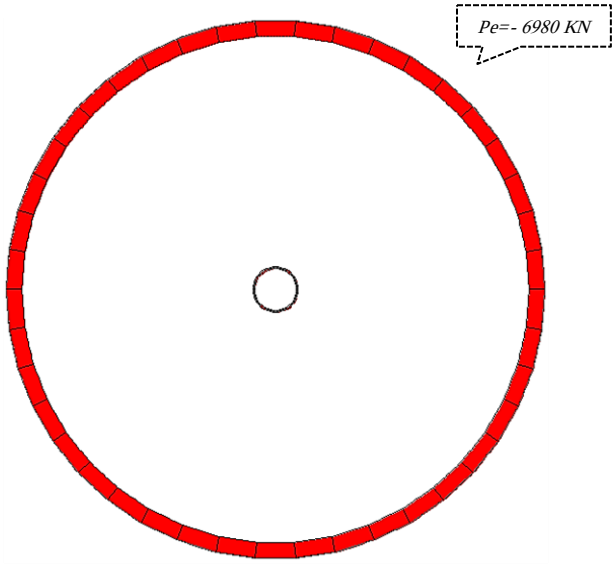

(b) Central ring tensions and edge ring compression

Fig. 5. Sketches of normal forces due to the case of dead + live loads

With the following figures, Figs. 6 to 13, the following symbols are used to define the cable curvature case:

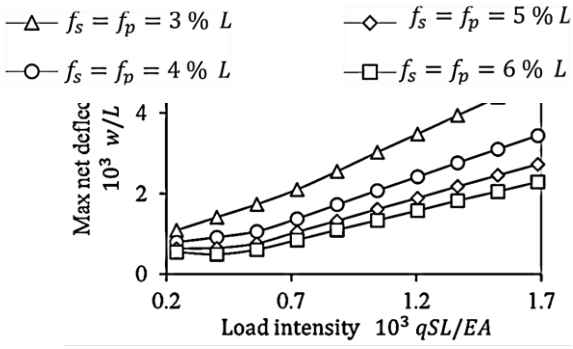

Fig. 6. Variation of maximum net deflections with cables curvature and load intensities

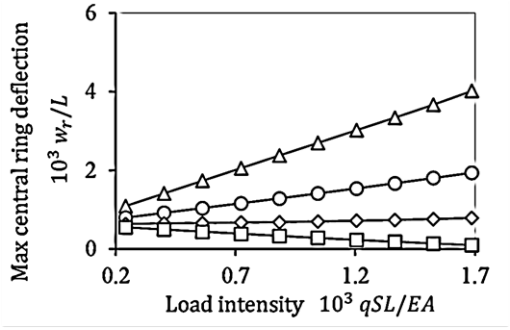

Fig. 7. Variation of central ring deflections with cables curvature and load intensities

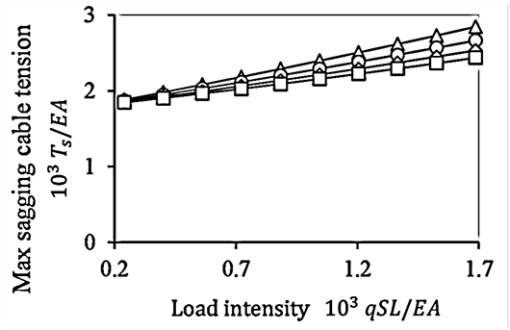

Fig. 8. Variation of sagging cable tensions with cables curvature and load intensities

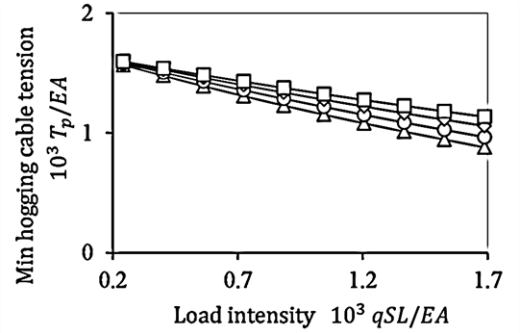

Fig. 9. Variation of hogging cable tensions with cables curvature and load intensities

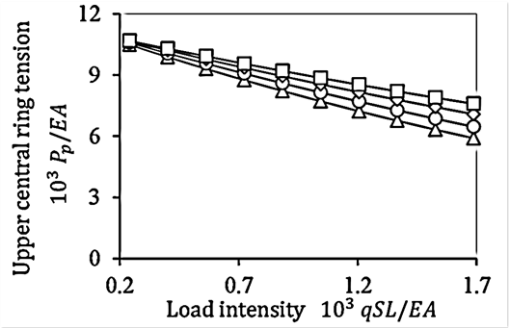

Fig. 10. Variation of upper central ring tensions with cables curvature and load intensities

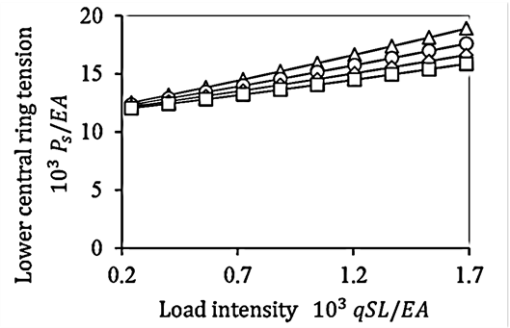

Fig. 11. Variation of lower central ring tensions with cables curvature and load intensities

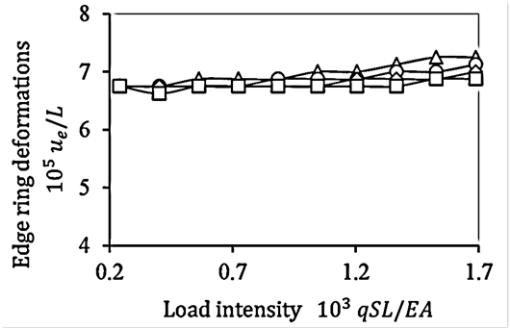

Fig. 12. Variation of edge ring deformations with cables curvature and load intensities

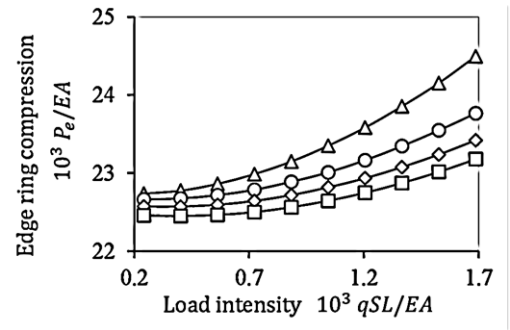

Fig.13. Variation of edge ring compression forces with cables curvature and load intensities

B. Effect of cable sizes on the response

In the latter, the analysis is carried out under the load combination of dead + live loads with a uniform intensity of q = 900 N/m^2. The same cable roof is reanalyzed for varying cable sizes ranged from EA = 83 MN to 680 MN. Three cases are considered as; Case (1): the extensional rigidity of hogging cables is kept constant at 297.7 MN, while that of sagging cables are varied, Case (2): the extensional rigidity of sagging cables are kept constant at 297.7 MN, while that of hogging cables are varied, Case (3): both of the extensional rigidity of hogging cables and sagging cables are varied.

With reference to Figs. 14 to 19. We can shortly note that:

1. Increasing sizes of both the hogging cables and/or the sagging cables, results a decrease of the maximum deflections of the net.
2. For Cases (2) and (3), increasing of cable sizes leads to reduce the hogging cable tensions, deformations and compression forces of the edge ring. On the other hand, increasing of cable sizes in Case (1) causes an increase on the same parameters.
3. Sagging cable tensions slightly increase with increasing of cable sizes in Cases (1) and (3), while they decrease with increasing cable sizes in Case (2).

With the following figures, Figs. 14 to 19, the following symbols are used to define the cable size case:

Case (1): $E_pA_p/H = 523$ & $E_sA_s/H = variable$

Case (2): $E_sA_s/H = 523$ & $E_pA_p/H = variable$

Case (3): $E_sA_s/H = E_pA_p/H = variable$

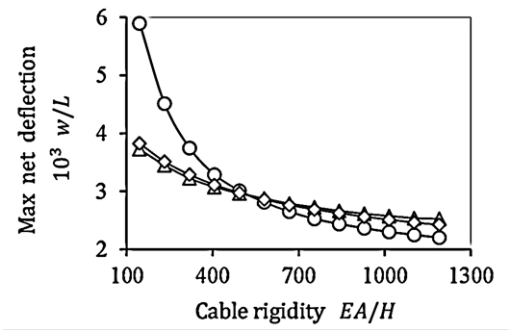

Fig. 14. Variation of maximum net deflections with cable sizes

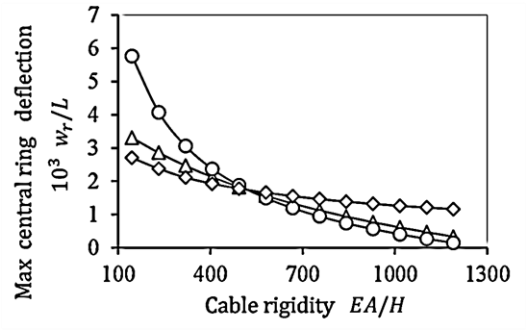

Fig. 15. Variation of central ring deflections with cable sizes

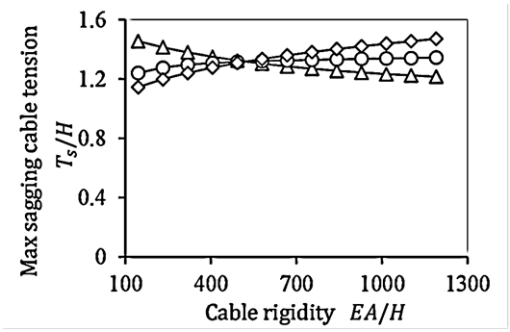

Fig. 16. Variation of sagging cable tensions with cable sizes

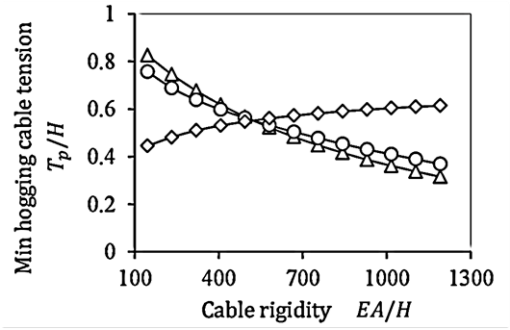

Fig. 17. Variation of hogging cable tensions with cable sizes

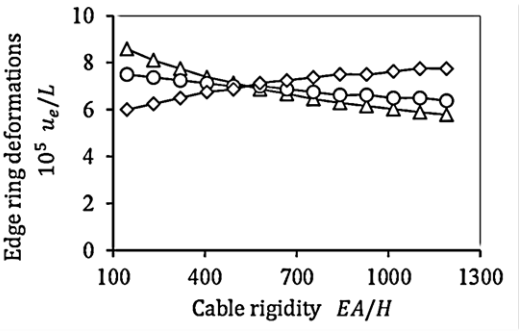

Fig. 18. Variation of edge ring deformations with cable sizes

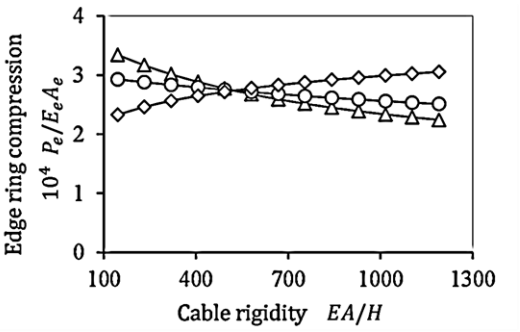

Fig. 19. Variation of edge ring compression forces with cable sizes

C. Effect of cable pretension forces on the response

Selecting the appropriate level of pretension is essential to keep cables always in tension and never become slack to avoid large deformations and formation of flat regions and fluttering due to unsatisfactory stiffness under any load combination [18].

The cable roof is analyzed for three levels of varying pretension forces ranged from H = 300 to 1200 KN. Level (1): the pretension forces of hogging cables are kept constant at 570 KN, while that of sagging cables are varied, Level (2): the pretension forces of sagging cables are kept constant at 570 KN, while that of hogging cables are varied, Level (3): both of the pretension forces of hogging cables and sagging cables are varied.

Results of the analysis are plotted in Figs. 20 to 25. Where, the following symbols are used to define the pretension force level:

—△— Level(1): $H_p/E_pA_p = 1.9 \times 10^{-3}$ & $H_s/E_sA_s = variable$

—○— Level(2): $H_s/E_sA_s = 1.9 \times 10^{-3}$ & $H_p/E_pA_p = variable$

—◇— Level(3): $H_s/E_sA_s = H_p/E_pA_p = variable$

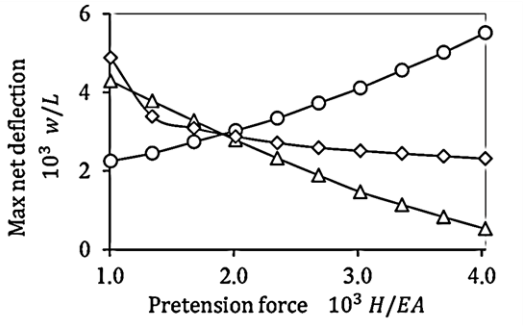

Fig. 20. Variation of maximum net deflections with cable pretension forces

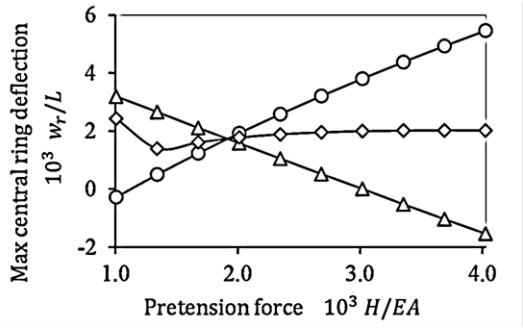

Fig. 21. Variation of central ring deflections with cable pretension forces

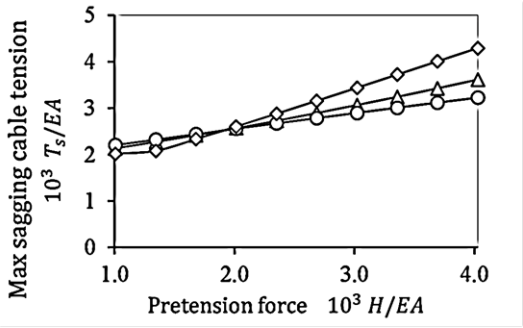

Fig. 22. Variation of sagging cable tensions with cable pretension forces

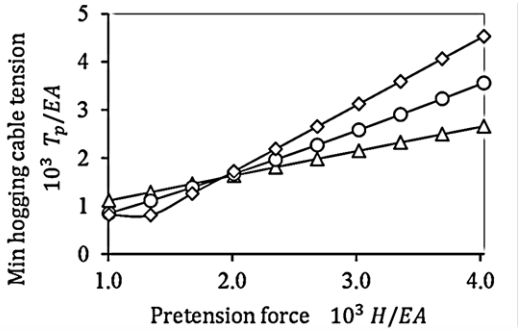

Fig. 23. Variation of hogging cable tensions with cable pretension forces

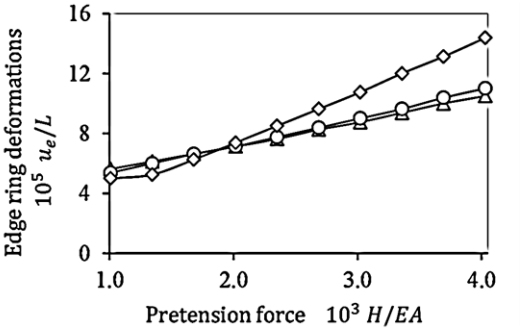

Fig. 24. Variation of edge ring deformations with cable pretension forces

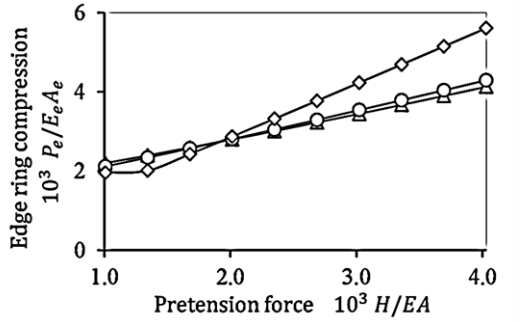

Fig. 25. Variation of edge ring compression forces with cable pretension forces

Generally, increasing of the cable size or its pretension force beyond the required values that keep cables always in tension without slacking causes a defect of utilizing of the cable cross-sectional area and lessen the effect of the pretension force. Hence, it is recommended that the design of cables and their cross-sectional areas are such that the maximum load the cables are expected to carry is less than or equal to 50% of their breaking strength, [19]. With reference to Figs. 20 to 25, it is noted that:

1. For Level (1), as the pretension forces of the sagging cables increase, the values of compression forces of the edge ring increase, on the other hand, the maximum deflections of the net decrease and the cable tensions are increased.
2. For Level (2), as the pretension forces of the hogging cables increase, the values of compression forces of the edge ring increase, also, the maximum deflection of the net and the cable tensions are increased.
3. Level (3) generally provides larger values of cable tensions and compression forces of the edge ring.

D. Effect of the stiffness of central rings and the diameters ratio on the response

In case of utilizing radial cable roofs, existence of tension rings leads to a more uniform distribution of cables, allows to use cable units with equal lengths, and reduces the number of cable terminals required. Figs. 26 to 31, show the effect of increasing the stiffness of both upper and lower central rings, E_rA_r = 1230 MN to 19700 MN, on the response for two values of the diameters ratio δ = 8% and 25%.

It is observed that, although varying of the stiffness and the diameters ratio affect the radial and vertical deformations of the central rings, it has marginal effects on the subsequent deformations and internal forces of other net elements.

The following symbols are used with Figs. 26 to 31, to define the diameters ratio used:

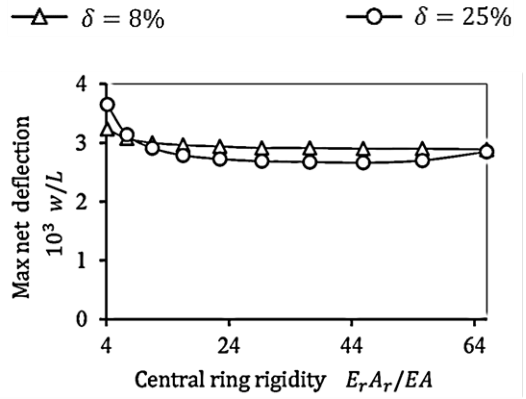

Fig. 26. Variation of net deflections with central rings stiffness and diameters ratio.

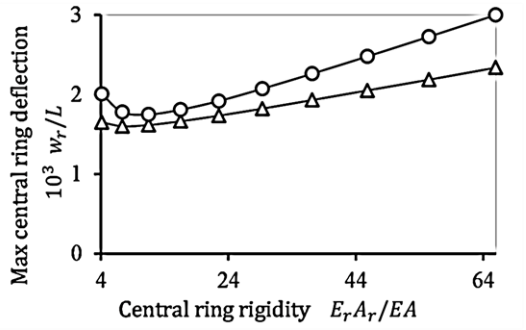

Fig. 27. Variation of central ring deflections with central rings stiffness and diameters ratio.

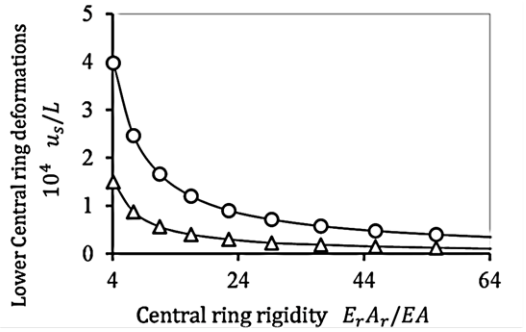

Fig. 28. Variation of lower central ring deformations with central rings stiffness and diameters ratio.

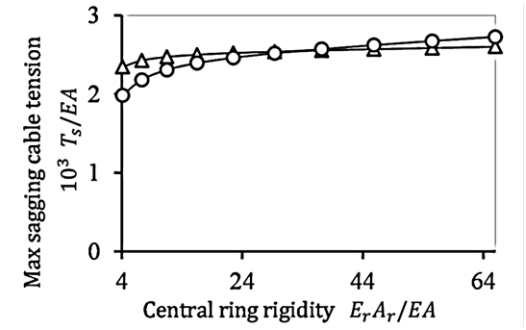

Fig. 29. Variation of sagging cable tensions with central rings stiffness and diameters ratio.

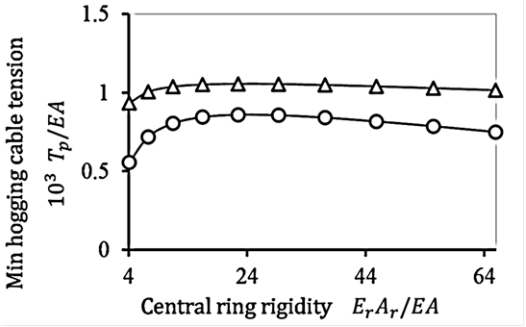

Fig. 30. Variation of hogging cable tensions with central rings stiffness and diameters ratio.

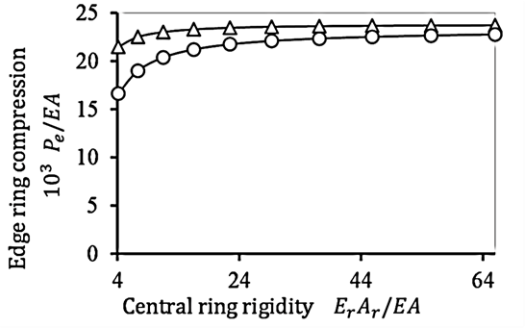

Fig. 31. Variation of edge ring compression forces with central rings stiffness and diameters ratio.

E. Effect of the stiffness of the boundary structure on the response

Figs. 32 to 38, show results due to the variation of edge ring stiffness, E_eA_e = 2295 to 36720 MN for three values of load intensities q = 500, 650, and 900 N/m^2.While in Figs. 39 to 45, the effects of column stiffness E_cA_c = 10000 to 68340 MN on the response are presented for three values of edge ring stiffness E_eA_e = 2295, 6699, and 36720 MN. The main features of the results are as follows:

1. The edge ring responses in a nonlinear manner due to the nonlinear behavior of the cables, which in turn greatly affects the response of the columns especially in case of low stiffness values of the edge beam.
2. The stiffness of a cable beam decreases with increasing flexibility and movements of the supporting system. When the supporting boundary is less stiff, as in case of cable ends not fixed but attached to elastic and deformable edge rings, the expected deflections are larger

and the corresponding cable tensions are smaller.

3. Therefore, as the stiffness of the edge ring increases, the resultant deformations of the net are decreased. At the same time, each of the maximum tension in cables, the tension force of central rings, the compression force of the edge ring, and the maximum bending moments of the of columns are decreased.
4. Column stiffness does not significantly influence the net response, but slightly affects the internal forces of the edge ring.

With the following figures, Figs. 32 to 38, the following symbols are considered to define the load intensity applied as:

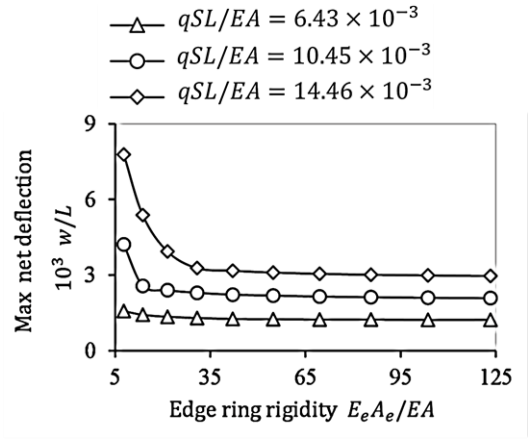

Fig. 32. Variation of net deflections with edge ring stiffness and load intensity.

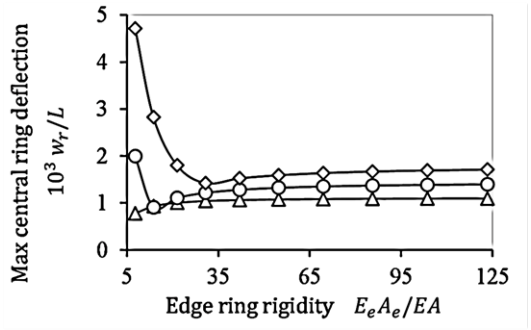

Fig. 33. Variation of central ring deflections with edge ring stiffness and load intensity.

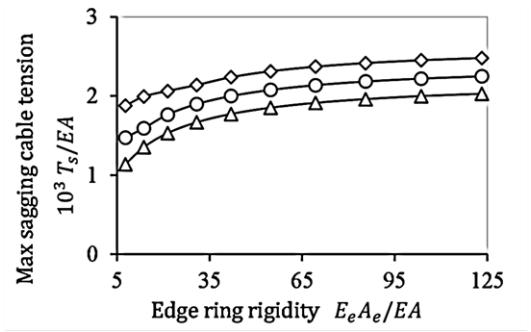

Fig. 34. Variation of sagging cable tensions with edge ring stiffness and load intensity.

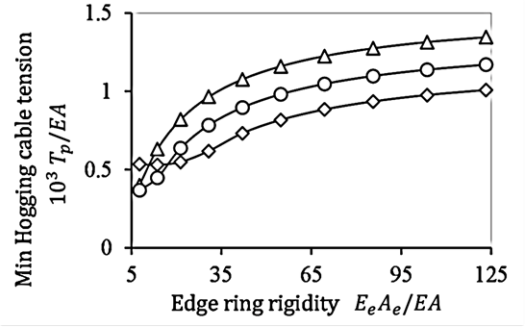

Fig. 35. Variation of hogging cable tensions with edge ring stiffness and load intensity.

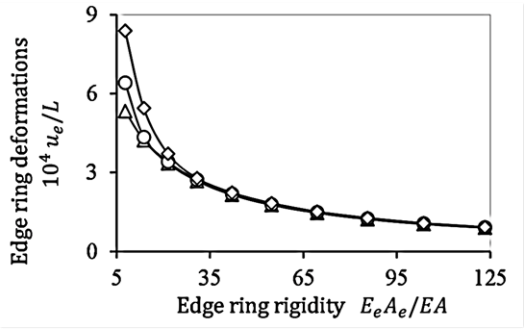

Fig. 36. Variation of edge ring deformations with edge ring stiffness and load intensity.

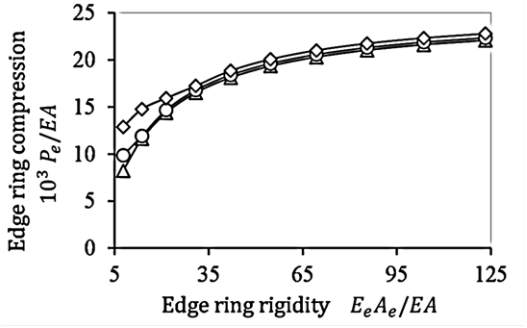

Fig. 37. Variation of edge ring compression forces with edge ring stiffness and load intensity.

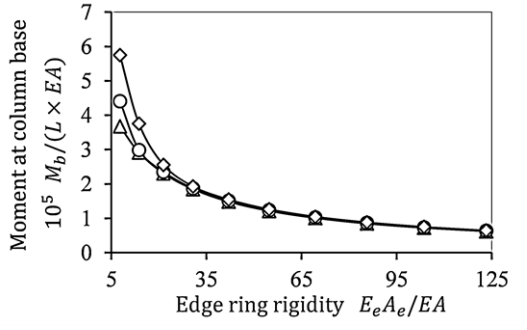

Fig. 38. Variation of moments at column base with edge ring stiffness and load intensity.

With the following figures, Figs. 39 to 45, the following symbols are used to indicate the utilized stiffness of the edge ring:

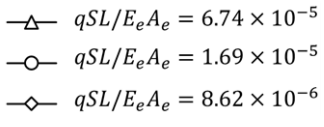

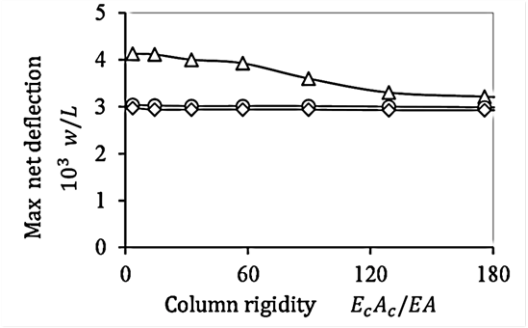

Fig. 39. Variation of net deflections with columns stiffness

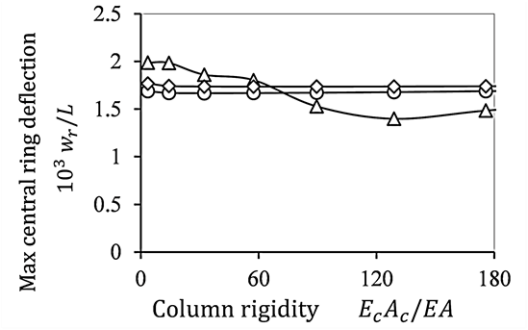

Fig. 40. Variation of central ring deflections with columns stiffness

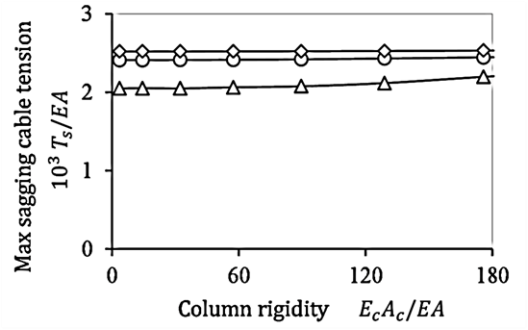

Fig. 41. Variation of sagging cable tensions with columns stiffness

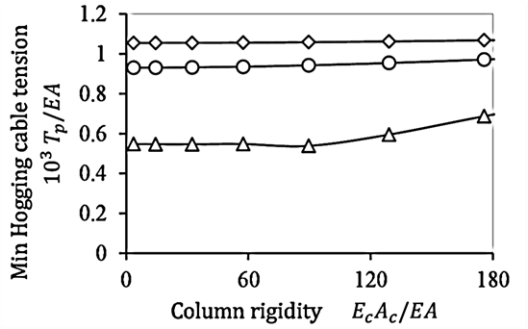

Fig. 42. Variation of hogging cable tensions with columns stiffness

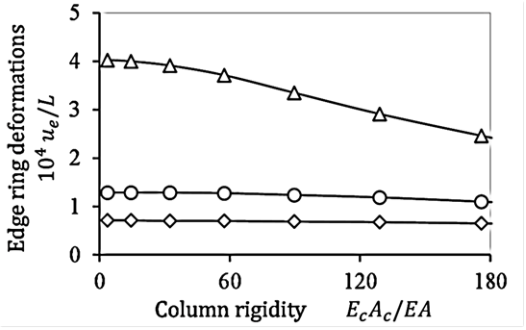

Fig. 43. Variation of edge ring deformations with columns stiffness

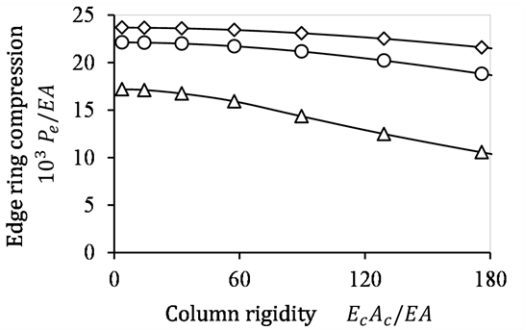

Fig. 44. Variation of edge ring compression forces with columns stiffness

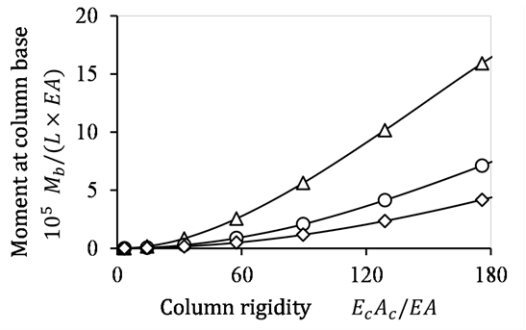

Fig. 45. Variation of moments at column base with columns stiffness

III. TRANSFORMATION RELATIONSHIPS

A well-known procedure used for preliminary design of suspension cable roofs has been presented by [20]. This method provides nondimensional graphs and tables constructed using a computer program based on the energy minimization approach. It can be used to obtain the nondimensional quantities for deflections, cable tensions and natural frequencies for several types of cable beams with rigid supports and subjected to uniformly distributed loads. The method suggested that:

1. Two systems have similar characteristics if: (i) the ratio of applying load to the cables extensional rigidity (qSl/EA) is constant, (ii) the sag/ rise to span ratios (f_s/L) and (f_p/L) are constant, and (iii) the ratio of pretension force to the

cables extensional rigidity (H/EA) is constant. Consequently their corresponding response is expected to be identical. Thus. (iv) The maximum deflection to span ratio (w/L) is constant, and (v) the ratio of maximum tension to the cables extensional rigidity (T_s/EA) is constant.

2. The preliminary design of the rings can be carried out by assuming that their normal forces are principally functions of the forces established by the horizontal components of the cable tensions. Therefore: (i) the tension of the upper central ring is directly proportional to the tension forces of the hogging cables($P_p \propto T_p$), (ii) the tension of the lower central ring is directly proportional to the tension forces of the sagging cables($P_s \propto T_s$), and (iii) the tension of the edge ring is directly proportional to the tension forces of both the hogging and sagging cables($P_e \propto T_p + T_s$).

According to these assumptions and in the progression of our work to achieve transformation relationships to account for the edge ring flexibility and the cables curvature. It is supposed that:

1. Since columns of radial cable networks only marginally affect their stiffness. In order to reduce the computational effort, each of, the *z*- displacements of the joints of the edge beam, the *x*- displacements for the two joints of the edge beam lie on the *x*-axis, and the y-displacements for the two joints of the edge beam lie on the *y*-axis were assumed to be restrained, so that the rigid body motion is prevented.
2. The proposed relationships are regarding the main characteristics that significantly influence the response of the network; and can be summarized in: (i) the extensional rigidity of the cables, where ($E_sA_s = E_pA_p = EA$), (ii) the cables curvature, where ($f_s/L = f_p/L = f/L$), (iii) the pretension force of the cables, where ($H_s = H_p = H$), (iv) the axial stiffness of the edge ring, (v)the maximum positive deflection of the net, (vi) the maximum and minimum tensions of the sagging and hogging cables (vii) the tensions forces of the upper and lower central rings, and (viii) maximum radial deformations and compression force of the edge ring.

The transformation relationships suggested for scaling of the prototype to the model with elastically deformable edge ring are presented. In the following *m* and *t* are subscripts point to the model and the prototype, respectively.

$$\left(\frac{qSL}{EA}\right)_m = \left(\frac{qSL}{EA}\right)_t \left(\frac{f_m / L_m}{f_t / L_t}\right)^2 \quad (1)$$

Maximum applied load to cable extensional rigidity ratio.

$$\left(\frac{H}{EA}\right)_m = \left(\frac{H}{EA}\right)_t \left(\frac{f_m / L_m}{f_t / L_t}\right)^2 \quad (2)$$

Pretension force to cable extensional rigidity ratio.

$$\left(\frac{E_eA_e}{EA}\right)_m = \left(\frac{E_eA_e}{EA}\right)_t \left(\frac{f_m / L_m}{f_t / L_t}\right)^2 \left(\frac{N_m}{N_t}\right) \quad (3)$$

Edge ring extensional rigidity to cable extensional rigidity ratio.

$$\left(\frac{E_rA_r}{EA}\right)_m = \left(\frac{E_rA_r}{EA}\right)_t \left(\frac{f_m / L_m}{f_t / L_t}\right)^2 \left(\frac{N_m}{N_t}\right) \quad (4)$$

Central ring extensional rigidity to cable extensional rigidity ratio.

$$\left(\frac{w}{L}\right)_m = \left(\frac{w}{L}\right)_t \quad (5)$$

Maximum net deflection to span ratio.

$$\left(\frac{u_e}{L}\right)_m = \left(\frac{u_e}{L}\right)_t \quad (6)$$

Maximum edge ring radial deformations to span ratio.

$$\left(\frac{T_s}{EA}\right)_m = \left(\frac{T_s}{EA}\right)_t \left(\frac{f_m / L_m}{f_t / L_t}\right)^2 \quad (7)$$

Maximum sagging cables tension to cable extensional rigidity ratio.

$$\left(\frac{T_p}{EA}\right)_m = \left(\frac{T_p}{EA}\right)_t \left(\frac{f_m / L_m}{f_t / L_t}\right)^{2.55} \quad (8)$$

Minimum hogging cables tension to cable extensional rigidity ratio.

$$\left(\frac{P_p}{EA}\right)_m = \left(\frac{P_p}{EA}\right)_t \left(\frac{f_m / L_m}{f_t / L_t}\right)^{2.55} \left(\frac{N_m}{N_t}\right) \quad (9)$$

Maximum upper central ring tension to cable extensional rigidity ratio.

$$\left(\frac{P_s}{EA}\right)_m = \left(\frac{P_s}{EA}\right)_t \left(\frac{f_m / L_m}{f_t / L_t}\right)^2 \left(\frac{N_m}{N_t}\right) \quad (10)$$

Maximum lower central ring tension to cable extensional rigidity ratio.

$$\left(\frac{P_e}{EA}\right)_m = \left(\frac{P_e}{EA}\right)_t \left(\frac{f_m / L_m}{f_t / L_t}\right)^2 \left(\frac{N_m}{N_t}\right) \quad (11)$$

Maximum edge ring compression to cable extensional rigidity ratio.

In order to verify the accuracy of the transformation relationships, several models are analyzed with different values of number of cable beams and sag/rise to span ratios. The analysis is carried out with keeping other parameters unchanged in both prototype and model. Table 3 shows the results from different analyses, based on a prototype of 42 cables, and several models with 10 to 80 cables with step of 10 cables.

The results obtained for the maximum tensions and deflections show that the model and the prototype are in excellent agreement. Also, Table 4 shows the results for a prototype with a sag/rise to span ratio of 4% and models with ratios between 4.5% and 6% with step 0.5%. In this case, the resulting error for maximum tensions was within -8% and -3%

while that for deflections was within -2% and -1%.

TABLE 3
CONVEX CABLE BEAMS, (SAG=RISE): MAXIMUM TENSIONS AND NET DEFLECTIONS FOR DIFFERENT NUMBER OF CABLE BEAMS
$qSL/EA = 2.15\times10^{-3}$

	Number of cable beams ***N***	**Net deflection** 10^3 ***w/L***	**Max cable tension** 10^3 ***Ts/EA***
Prototype	**42**	**4.3250**	**3.1686**
Model	10	4.3375	3.1679
Model	20	4.3250	3.1701
Model	30	4.3250	3.1691
Model	40	4.3250	3.1687
Model	50	4.3250	3.1684
Model	60	4.3250	3.1689
Model	70	4.3250	3.1683
Model	80	4.3250	3.1684

TABLE 4
CONVEX CABLE BEAMS, (SAG=RISE): MAXIMUM TENSIONS AND NET DEFLECTIONS FOR DIFFERENT CABLES CURVATURE
$qSL/EA = 2.0\times10^{-3}$

	Sag/Rise ***f/L***	**Net deflection** 10^3 ***w/L***	**Max cable tension** 10^3 ***Ts/EA***
Prototype	**4%**	**4.1625**	**2.9683**
Model	**4.5%**	4.1375	2.8895
Model	**5%**	4.1125	2.8276
Model	**5.5%**	4.1125	2.7778
Model	**6%**	4.1000	2.7370

IV. PRELIMINARY ANALYSIS GRAPHS AND ILLUSTRATIVE EXAMPLES

The 80m model previously illustrated in section II again is analyzed for the construction of the graphs. In this analysis, sizes and pretension forces for both the sagging and the hogging cables are kept equal. All cable sizes are assumed according to ASTM: A586 − 04a standards [21], with nominal diameters ranged from 30mm to 63.5mm in order to have a range of cable extensional rigidity from 100 to 400 MN.

The supposed load intensities and the pretension are taken as percentage of the cable extensional rigidity. The study is carried out for a wide range of load intensities, $qSL/EA = 0.25\times10^{-3}$ to 5×10^{-3}, and pretension forces, $H/EA = 1\times10^{-3}$ to 5×10^{-3}.

Graphs achieved are dimensionless and can be applied for all systems of units. They provide the maximum and minimum tensions, maximum positive deflections of the net, and maximum normal forces and deformations of rings (Figs. 46 to 49) for E_eA_e/EA = 125 to 500. Also, values of the same nondimensional parameters mentioned above are tabulated in Tables 9 to 12.

When the preliminary graphs were constructed, the outcomes of the response in the state in which the final tensions in part of hogging cables are approaching to zero were eliminated. In order to provide accurate and precise results. Whereas, the loss of the tensile strength in the cables causes the net to be unstable. This occurs significantly when the load is greater than the pretension force.

A. ILLUSTRATIVE EXAMPLE (1)

In order to demonstrate the use of the non-dimensional diagrams and tables given in this paper, the preliminary design calculations for a 100 m diameter circular cable roof with radial convex cable beams with design parameters given as shown under the first column of Table 5.

TABLE 5
PROPERTIES OF CABLES UTILIZED IN THE PARAMETRIC STUDY

Parameters	Example (1)	Example (2)
Net diameter, *L* (m)	100	60
Sag=Rise, *f/L* (%)	4%	5%
Load intensity, *q* (KN/m^2)	1.0	1.15
Number of cable beams, *N*	56	36
Spacing between cable beams, S(m)	5.61	5.23
Cables extensional rigidity, *EA* (MN)	300	155
Pretension force, *H* (KN)	600	387.5
Edge ring extensional rigidity, *EeA*e(MN)	50000	35000

These prototype characteristics can be used to yield the nondimensional parameters of the model, for which the preliminary charts have been produced using equations (1 to 3). Hence:

$$\left(\frac{qSL}{EA}\right)_m = \left(\frac{1.0\times5.61\times100}{300000}\right)\times\left(\frac{4}{4}\right)^2 = 1.87\times10^{-3};$$

$$\left(\frac{H}{EA}\right)_m = \frac{600}{300000}\times\left(\frac{4}{4}\right)^2 = 2\times10^{-3}; \text{ and}$$

$$\left(\frac{E_eA_e}{EA}\right)_m = \frac{50000}{300}\times\left(\frac{4}{4}\right)^2\times\left(\frac{42}{56}\right) = 125$$

Using preliminary curves of Fig. 46 for $E_eA_e/EA = 125$, the curve for $qSL/EA = 1.87\times10^{-3}$ can be plotted by interpolating the values of 1.5×10^{-3} and 2.0×10^{-3}. Using the resulting curves, the model responses can be derived as recorded under the first column of Table 6.

These values can be scaled back to the prototype using equations (5 to 11) as given below:

$w = 4.05\times10^{-3}\times100 = 405mm$;

$u_e = 1\times10^{-4}\times100 = 10mm$;

$T_s = 2.80\times10^{-3}\times300000 = 840KN$;

$T_p = 0.96\times10^{-3}\times300000 = 288KN$;

$P_p = 6.40\times10^{-3}\times300000\times\left(\frac{56}{42}\right) = 2560KN$;

$P_s = 18.46\times10^{-3}\times300000\times\left(\frac{56}{42}\right) = 7384KN$; and

$P_e = 24.56\times10^{-3}\times300000\times\left(\frac{56}{42}\right) = 9824KN$

TABLE 6
NONDIMENSIONAL PRELIMINARY RESPONSE OF THE MODELS USED IN THE ILLUSTRATIVE EXAMPLES

Response	Example (1)	Example (2)
w/L	4.05×10^{-3}	3.50×10^{-3}
ue/L	1.00×10^{-4}	6.00×10^{-4}
Ts/EA	2.80×10^{-3}	2.31×10^{-3}
Tp/EA	0.96×10^{-3}	0.79×10^{-3}
Pp/EA	6.40×10^{-3}	5.27×10^{-3}
Ps/EA	18.46×10^{-3}	15.26×10^{-3}
Pe/EA	24.60×10^{-3}	20.30×10^{-3}

In order to comprehend the proposed method, a nonlinear analysis of the prototype is carried out. Table. 7 shows that the results obtained from the proposed method are in great agreement with that obtained using SAP2000. Where, the accuracy is almost 97% for the net deflections, 99% for the cable maximum tensions, 92% for the cable minimum tensions, 92% and 99% for the upper and lower central rings tension forces respectively, and 98% for the edge ring compression force.

TABLE 7
RESULTS OF THE ANALYSIS OF THE PROTOTYPE USED IN ILLUSTRATIVE EXAMPLE (1)

Response	Present study	SAP2000	Minimization of T.P.E
Max deflection, *w* (mm)	405	393	394
Max sagging tension, *Ts* (KN)	840	849	848
Min hogging tension, *Tp* (KN)	288	267	268
Upper central ring tension, *Pp* (KN)	2560	2381	2386
Lower central ring tension, *Ps* (KN)	7384	7444	7456
Edge ring compression, *Pe*(KN)	9842	9641	9655

B. ILLUSTRATIVE EXAMPLE (2)

For the second case of study the prototype has a different curvature from the model with the characteristics presented under the second column of Table 5. The prototype parameters can be scaled to the model for which the preliminary charts have been produced by setting:

$$\left(\frac{qSL}{EA}\right)_m = \left(\frac{1.15\times5.23\times60}{155000}\right)\times\left(\frac{4}{5}\right)^2 = 1.50\times10^{-3}$$

$$\left(\frac{H}{EA}\right)_m = \frac{387.5}{155000}\times\left(\frac{4}{5}\right)^2 = 1.6\times10^{-3}$$

$$\left(\frac{E_eA_e}{EA}\right)_m = \frac{31250}{155}\times\left(\frac{4}{5}\right)^2\times\left(\frac{42}{36}\right) = 168$$

Using preliminary curves of Fig. 47 for *EeAe/EA* = 167, the model response can be determined as shown under the second column of Table 6. These values can be scaled back to the prototype using equations (5 to 11) similarly as in the previous example. Hence:

$w = 3.50\times10^{-3}\times60 = 210mm$;

$u_e = 6\times10^{-4}\times60 = 3.6mm$;

$T_s = 2.31\times10^{-3}\times155000\times\left(\frac{5}{4}\right)^2 = 559.45KN$;

$T_p = 0.79\times10^{-3}\times155000\times\left(\frac{5}{4}\right)^{2.55} = 216.31KN$;

$P_p = 5.27\times10^{-3}\times155000\times\left(\frac{36}{42}\right)\times\left(\frac{5}{4}\right)^{2.55} = 1236.85KN$;

$P_s = 15.26\times10^{-3}\times155000\times\left(\frac{36}{42}\right)\times\left(\frac{5}{4}\right)^2 = 3167.81KN$; and

$P_e = 20.30\times10^{-3}\times155000\times\left(\frac{36}{42}\right)\times\left(\frac{5}{4}\right)^2 = 4214.06KN$

Results due to nonlinear analyses and the preliminary method are given in Table 8. It is noted that, the accuracy is approximately 97% for the net deflections, 95% for the cable maximum tensions, 96% for the cable minimum tensions, 97% and 94% for the upper and lower central rings tension forces respectively, and 99% for the edge ring compression force.

TABLE 8
RESULTS OF THE ANALYSIS OF THE PROTOTYPE USED IN ILLUSTRATIVE EXAMPLE (2)

Response	Present study	SAP2000	Minimization of T.P.E
Max deflection, *w* (mm)	210	204	205
Max sagging tension, *Ts* (KN)	559.45	533	525
Min hogging tension, *Tp* (KN)	216.31	224	216
Upper central ring tension, *Pp* (KN)	1236.85	1280	1238
Lower central ring tension, *Ps* (KN)	3167.81	2984	2953
Edge ring compression, *Pe*(KN)	4214.06	4246	4143

TABLE 9
THE PRELIMINARY RESPONSE OF THE CONVEX CABLE BEAMS ROOF FOR SAG/RISE TO SPAN RATIO f= 4% L, LOAD INTENSITY $qSL/EA = 1.0\times10^{-3}$ to 3.0×10^{-3}, PRETENSION FORCE $H/EA = 1\times10^{-3}$ to 5×10^{-3}, EDGE RING RIGIDITY $EeAe/EA$ = 125.

Triangular distributed load, $qSL/EA = 1\times10^{-3}$

10^3 *H/EA*	10^3 *w/L*	10^3 *Ts/EA*	10^3 *Tp/EA*	10^3 *Pp/EA*	10^3 *Ps/EA*	10^3 *Pe/EA*
1	2.9875	1.5185	0.4437	2.9828	10.0222	12.8498
2	2.2125	2.2828	1.2827	8.5789	15.0837	23.3829
3	1.8625	3.1040	2.1681	14.4941	20.5164	34.5949
4	1.6750	3.9403	3.0578	20.4383	26.0403	45.9347
5	1.5625	4.7839	3.9473	26.3862	31.6174	57.3170

Triangular distributed load, $qSL/EA = 2\times10^{-3}$

2	4.3125	2.8765	1.0916	6.1076	18.9866	24.7880
3	3.6750	3.6235	1.6157	11.9488	23.9226	35.4591
4	3.2875	4.4108	2.5179	17.9713	29.1207	46.5415
5	3.0500	5.2177	3.4278	24.0136	34.4569	57.7812

Triangular distributed load, $qSL/EA = 3\times10^{-3}$

3	5.4125	4.1713	1.4545	9.7128	27.5277	36.7969
4	4.8750	4.9044	2.3545	15.7355	32.3587	47.5285
5	4.5375	5.6697	3.2692	21.8354	37.4094	58.5515

TABLE 10
THE PRELIMINARY RESPONSE OF THE CONVEX CABLE BEAMS ROOF FOR SAG/RISE TO SPAN RATIO f= 4% L, LOAD INTENSITY $qSL/EA = 1.0\times10^{-3}$ to 3.0×10^{-3}, PRETENSION FORCE $H/EA = 1\times10^{-3}$ to 5×10^{-3}, EDGE RING RIGIDITY $EeAe/EA$ = 167.

Triangular distributed load, $qSL/EA = 1\times10^{-3}$

10^3 *H/EA*	10^3 *w/L*	10^3 *Ts/EA*	10^3 *Tp/EA*	10^3 *Pp/EA*	10^3 *Ps/EA*	10^3 *Pe/EA*
1	2.9125	1.5437	0.4733	3.1695	10.1942	13.2012
2	2.1625	2.3395	1.3434	8.9820	15.4614	24.1555
3	1.8250	3.1903	2.2584	15.1031	21.0903	35.7611
4	1.6250	4.0560	3.1785	21.2497	26.8032	47.4900
5	1.5125	4.9289	4.0973	27.3846	32.5769	59.2598

Triangular distributed load, $qSL/EA = 2\times10^{-3}$

2	25.5412	2.9298	0.9734	6.5032	19.3391	25.5412
3	36.6081	3.7063	1.8810	12.5718	24.4746	36.6081
4	48.0967	4.5229	2.8120	18.7963	29.8679	48.0967
5	59.7236	5.3582	3.7470	25.0416	35.3915	59.7236

Triangular distributed load, $qSL/EA = 3\times10^{-3}$

3	5.2875	4.2509	1.5488	10.3489	28.0443	37.9453
4	4.7625	5.0128	2.4805	16.5628	33.0846	49.0711
5	4.4250	5.8075	3.4242	22.8758	38.3367	60.4835

TABLE 11
THE PRELIMINARY RESPONSE OF THE CONVEX CABLE BEAMS ROOF FOR SAG/RISE TO SPAN RATIO f= 4% L, LOAD INTENSITY qSL/EA = 1.0×10^{-3} to 3.0×10^{-3}, PRETENSION FORCE H/EA = 1×10^{-3} to 5×10^{-3}, EDGE RING RIGIDITY $EeAe/EA$ = 250.

Triangular distributed load, qSL/EA = 1×10^{-3}

10^3 H/EA	10^3 w/L	10^3 Ts/EA	10^3 Tp/EA	10^3 Pp/EA	10^3 Ps/EA	10^3 Pe/EA
1	2.8500	1.5727	0.5038	3.3702	10.3847	13.5940
2	2.1125	2.4006	1.4079	9.4131	15.8643	24.9813
3	1.7750	3.2827	2.3549	15.7522	21.7048	37.0088
4	1.5875	4.1793	3.3069	22.1181	27.6280	49.1576
5	1.4750	5.0838	4.2577	28.4653	33.6076	61.3434

Triangular distributed load, qSL/EA = 2×10^{-3}

1	7.3625	2.6632	0.8666	5.9533	17.6898	23.1051
2	4.1250	2.9869	1.0393	6.9434	19.7154	26.3497
3	3.5000	3.7958	1.9801	13.2336	25.0651	37.8449
4	3.1375	4.6436	2.9440	19.6744	30.6673	49.7521
5	2.9000	5.5101	3.9115	26.1389	36.3961	61.8032

Triangular distributed load, qSL/EA = 3×10^{-3}

3	5.1625	4.3361	1.6502	11.0219	28.6102	39.1744
4	4.6625	5.1300	2.6146	17.4762	33.8659	50.7282
5	4.3125	5.9554	3.5912	24.0043	39.3209	62.5730

TABLE 12
THE PRELIMINARY RESPONSE OF THE CONVEX CABLE BEAMS ROOF FOR SAG/RISE TO SPAN RATIO f= 4% L, LOAD INTENSITY qSL/EA = 1.0×10^{-3} to 3.0×10^{-3}, PRETENSION FORCE H/EA = 1×10^{-3} to 5×10^{-3}, EDGE RING RIGIDITY $EeAe/EA$ = 500.

Triangular distributed load, qSL/EA = 1×10^{-3}

10^3 H/EA	10^3 w/L	10^3 Ts/EA	10^3 Tp/EA	10^3 Pp/EA	10^3 Ps/EA	10^3 Pe/EA
1	2.7875	1.6037	0.5367	3.5938	10.5930	14.0125
2	2.0625	2.4657	1.4772	9.8785	16.2954	25.8672
3	1.7250	3.3815	2.4594	16.4430	22.3491	38.3445
4	1.5375	4.3126	3.4452	23.0431	28.5156	50.9499
5	1.4250	5.2500	4.4297	29.6209	34.7146	63.5798

Triangular distributed load, qSL/EA = 2×10^{-3}

1	7.0625	2.6838	0.8687	5.9635	17.8379	23.2456
2	4.0250	3.0489	1.1094	7.4155	20.1289	27.2215
3	3.4125	3.8910	2.0863	13.9506	25.7022	39.1747
4	3.0625	4.7724	3.0851	20.6262	31.5383	51.5375
5	2.8250	5.6726	4.0871	27.3253	37.4874	64.0394

Triangular distributed load, qSL/EA = 3×10^{-3}

3	5.0375	4.4282	1.7582	11.7438	29.2251	40.4936
4	4.5500	5.2557	2.7579	18.4282	34.6996	52.5045
5	4.2125	6.1145	3.7697	25.1977	40.3830	64.8010

The following symbols are used to indicate the pretention forces for Figs. 46 to 49:

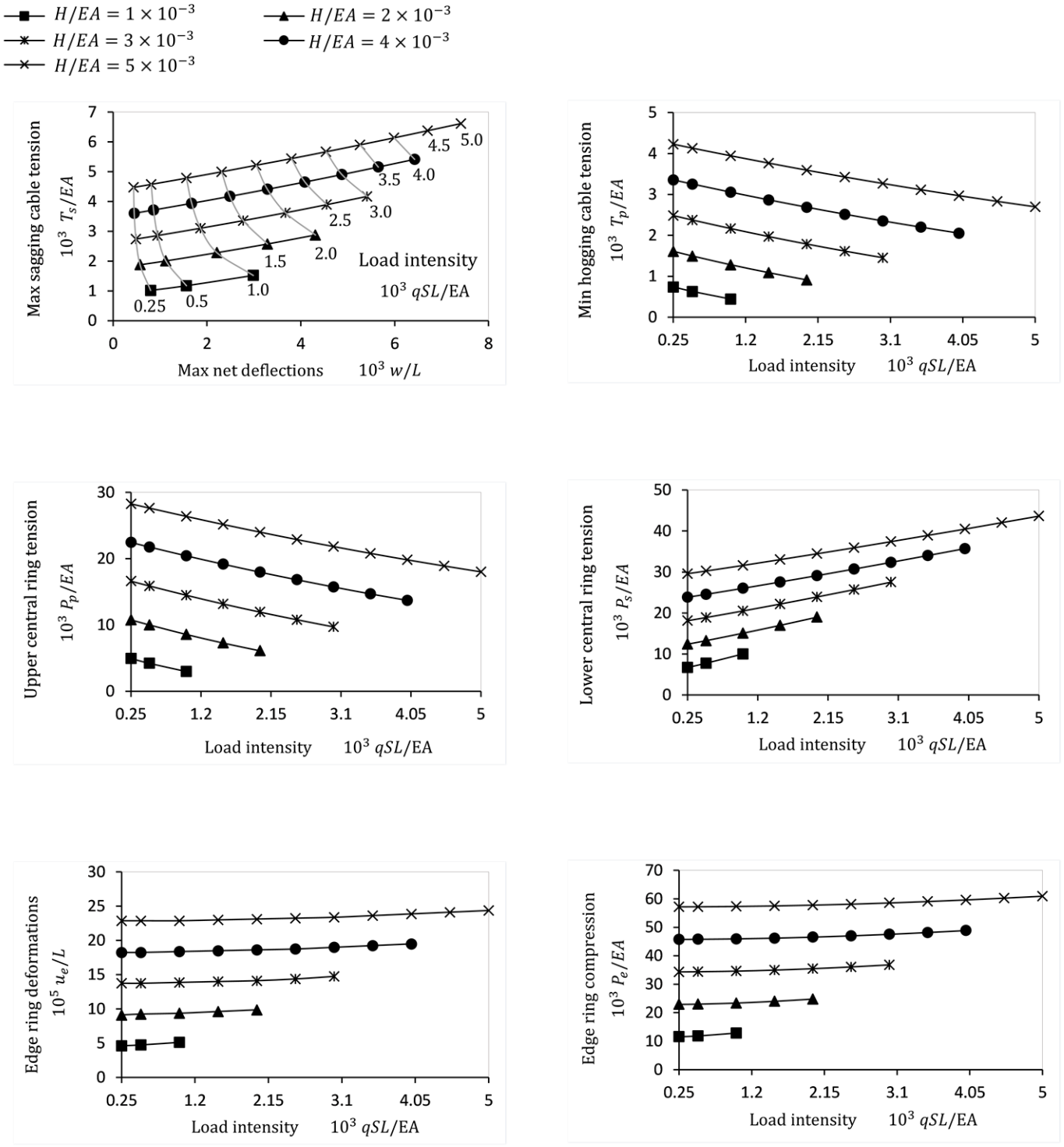

Fig. 46. Response of the convex cable roof beams, for sag/rise to span ratio f= 4% L, load intensity qSL/EA= 0.25×10^{-3} to 5×10^{-3}, pretension force H/EA= 1×10^{-3} to 5×10^{-3}, and edge ring rigidity $EeAe/EA$= 125.

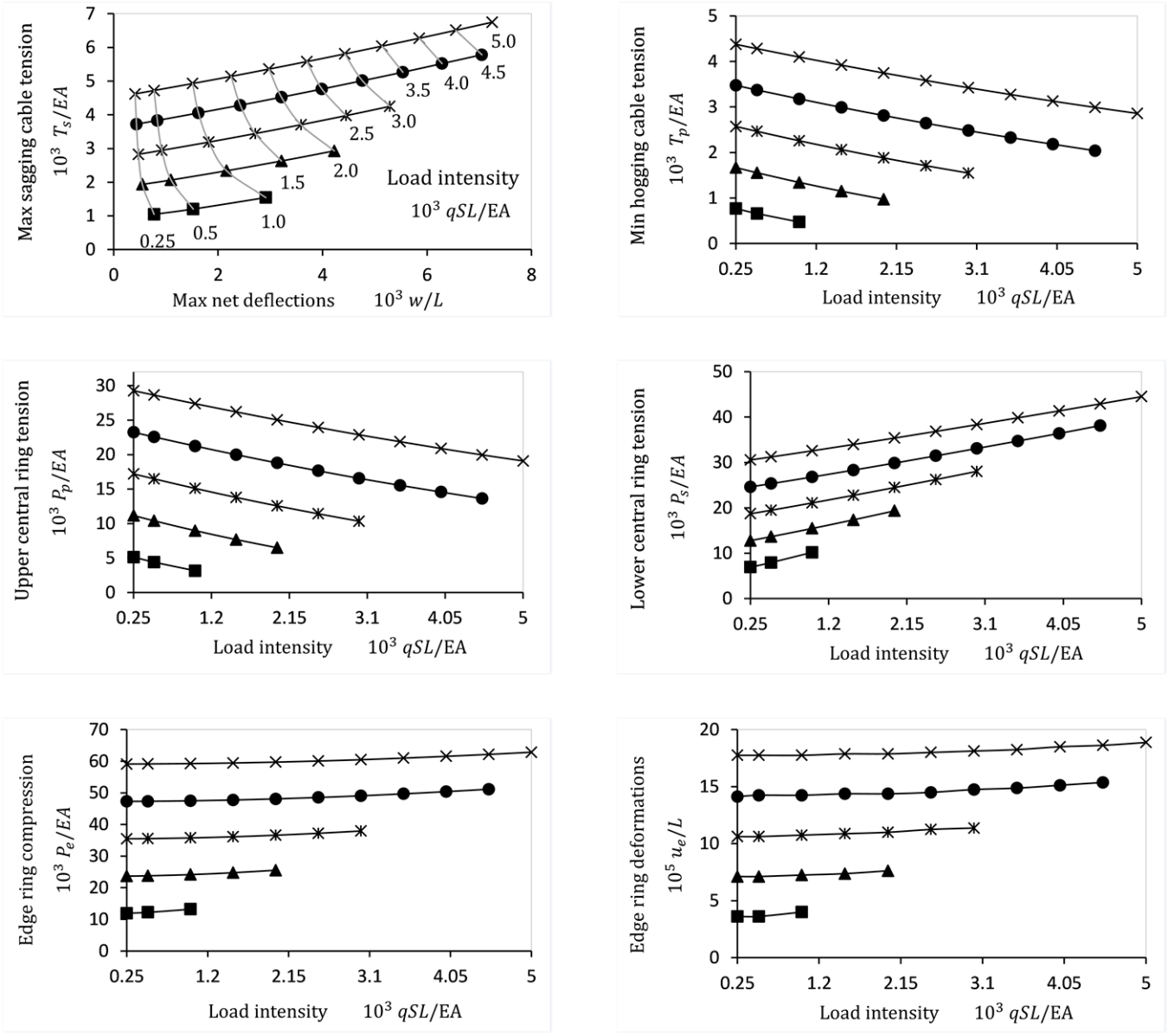

Fig. 47. Response of the convex cable roof beams, for sag/rise to span ratio f= 4% L, load intensity qSL/EA= 0.25×10^{-3} to 5×10^{-3}, pretension force H/EA = 1×10^{-3} to 5×10^{-3}, and edge ring rigidity $EeAe/EA$= 167.

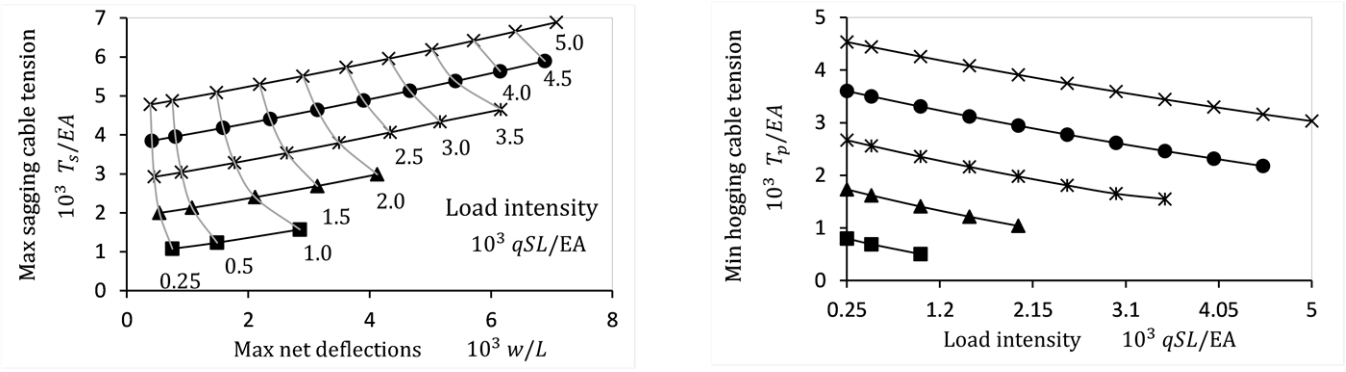

Fig. 48. Response of the convex cable roof beams, for sag/rise to span ratio f= 4% L, load intensity qSL/EA= 0.25×10^{-3} to 5×10^{-3}, pretension force H/EA = 1×10^{-3} to 5×10^{-3}, and edge ring rigidity $EeAe/EA$= 250.

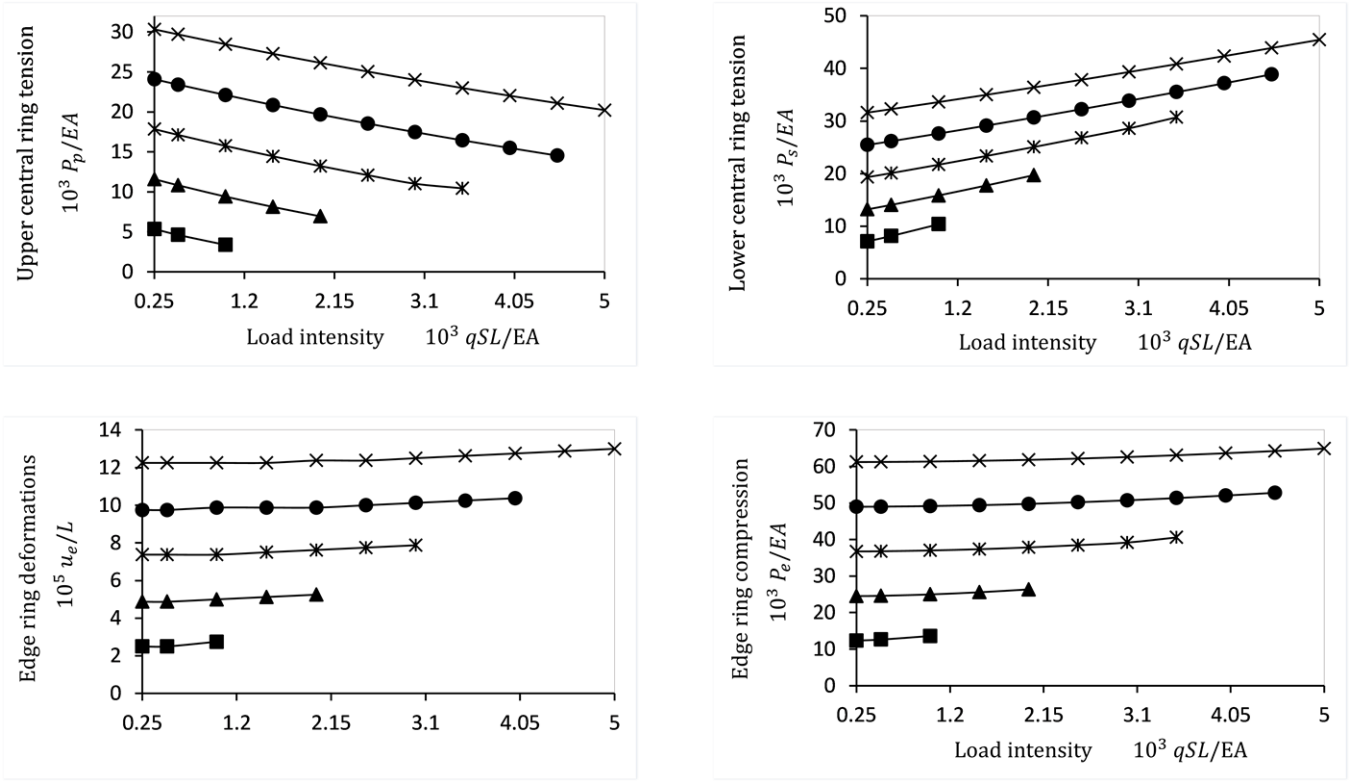

Fig. 48. Continued

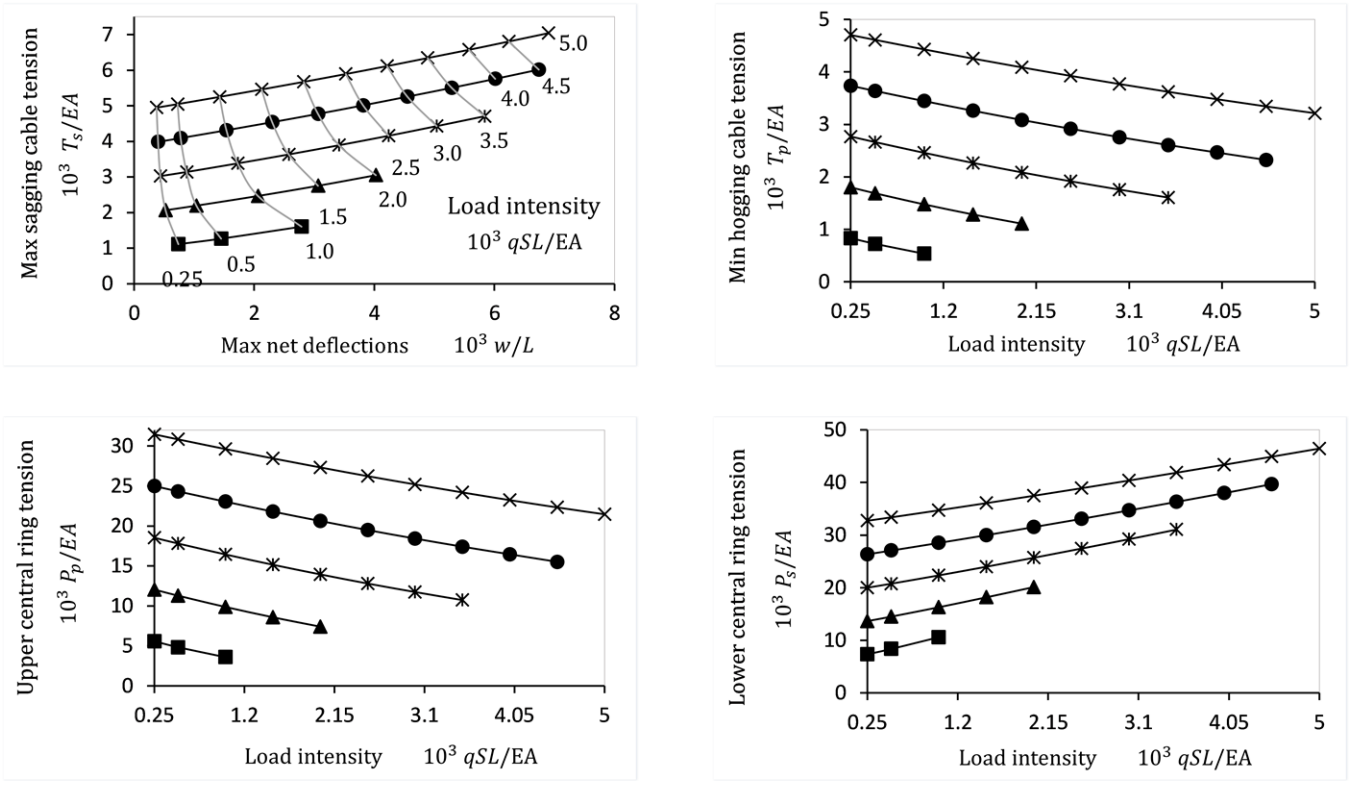

Fig. 49. Response of the convex cable roof beams, for sag/rise to span ratio $f = 4\%\ L$, load intensity $qSL/EA = 0.25\times10^{-3}$ to 5×10^{-3}, pretension force $H/EA = 1\times10^{-3}$ to 5×10^{-3}, and edge ring rigidity $EeAe/EA = 500$.

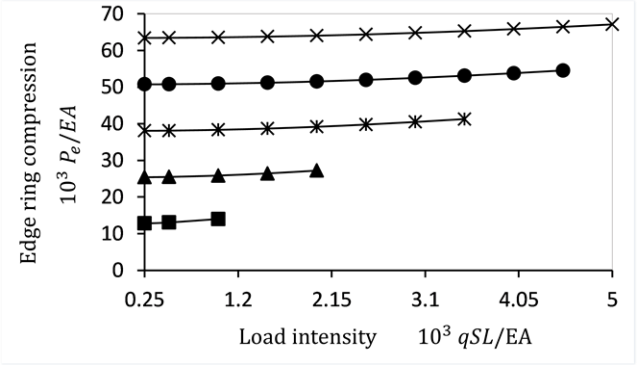

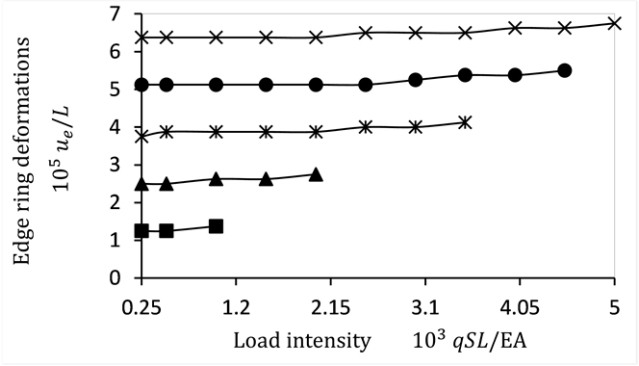

Fig. 49. Continued

V. SYMMARY AND CONCLUSION

This paper includes a study of the response of cable systems with deformable supports to present a preliminary analysis approach that has been examined and verified. It may be concluded that:

1. The stiffness of the sagging cables and curvature of hogging cables have a significant effects.
2. Although preliminary methods and simplifications that impose the supports of cable nets are infinite rigid give reasonable results. The stiffness of the edge ring must be included in the analysis.
3. It is essential to carry out a geometrically nonlinear static analysis in order to efficiently design cable structures, since the nonlinear behavior of the cables greatly affects the response of the rings which consequently behave in nonlinear manner.

NOTATIONS

q = Equivalent load intensity per unit area due to any load combination (dead, live, wind, …., etc.)
$q_s = q \times S$ The maximum load intensity per meter run on a cable beam.
L = the roof diameter.
l = central ring diameter.
$\delta = l/L$ = the diameters ratio.
N = number of convex cable beams.
S = span between convex cable beams= $\pi \times L / N$.
f_p = hogging cable rise.
f_s = sagging cable sag.
H_p = hogging cable pretension force.
H_s = sagging cable pretension force.
E_pA_p = extensional rigidity of hogging cable.
E_sA_s = extensional rigidity of sagging cable.
E_vA_v = extensional rigidity of separator struts.
E_rA_r = extensional rigidity of central rings.
E_eA_e = extensional rigidity of the edge ring.
E_cA_c = extensional rigidity of columns.
MN = Mega Newton.

REFERENCES

[1] H. T. Thai and S. E. Kim, "Nonlinear static and dynamic analysis of cable structures," *Finite elements in analysis and design*, vol. 47, no. 3, pp. 237-246, 2011.
[2] W. J. Lewis, M. S. Jones, and K. R. Rushton, "Dynamic relaxation analysis of the non-linear static response of pretensioned cable roofs," *Computers & Structures*, vol. 18, no. 6, pp. 989-997, 1984.
[3] E. Coarita and L. Flores, "Nonlinear analysis of structures cable-truss," *International Journal of Engineering and Technology*, vol. 7, no. 3, pp. 160, 2015.
[4] C. C. Lai, "Static analysis of prestressed cable networks," Ph.D. thesis, Dept. Civil Eng., Kansas State Univ., Manhattan, Kansas, 1973.
[5] Y. M. Desai and S. Punde, "Simple model for dynamic analysis of cable supported structures," *Engineering Structures*, vol. 23, no. 3, pp. 271-279, 2001.
[6] J. S. Gero, "The preliminary design of cable network structures," Structures Report SR9, University of Sydney, 1975.
[7] W.J. Lewis, "Introduction," in *Tension structures: form and behavior*, London: Thomas Telford, 2003, pp. 1-20.
[8] I. Talvik, "The finite element modeling of cable networks with flexible support," *Computers and Structures*, vol. 79, pp. 2443-2450, 2001.
[9] M. Majowiecki and F. Zoulas, "The elastic interaction between the rope net and space frame anchorage structures," in *Proc. the International Conference of Space Structures*, 1984, pp. 778-784.
[10] J. Szabó, L. Kollár, and M. V. Pavlovic, *Structural design of cable suspended roofs*, England: Howard Limited, 1984.
[11] I. Vassilopoulou and C.J. Gantes, "Cable nets with elastically deformable edge ring," *International Journal of Space Structures*, vol. 20, no. 1, pp. 15-34, 2005.
[12] M. Naguib, S. El Bagalaty, and S. Selim, "Optimum design of concave cable roofs," Mansoura Engineering Journal, vol. 21, no. 1, 1996.
[13] SAP2000, *CSI Analysis Reference Manual*, Computer and Structures, Berkeley, 2010.
[14] K. SANTOSO, "Wide-span cable structures," Ph.D., Thesis, Dept. Civil and Environmental Eng., Massachusetts Institute of Technology, Cambridge, Massachusetts, 2004.
[15] P. Krishna, "Analysis of pretensioned cable systems," in *Cable-suspended roofs*, New York: McGraw-Hill Companies, 1978 pp. 55-115.
[16] A. Pintea, and G. Tarta, "Comparison between the linear and nonlinear responses of cable structures II–dynamic loading," *Procedia. Engineering*, vol. 40, pp. 375-380, 2012.
[17] M. Mohie-Eldin, M.S. thesis, "Static and dynamic analysis of circular cable suspended roofs," Dept. Civil. Eng., Mansoura Univ., Egypt, 2003.
[18] I. Vassilopoulou, F. Petrini, and C.J. Gantes, "Nonlinear Dynamic Behavior of Cable Nets Subjected to Wind Loading," *Elsevier. Structures*, vol. 10, pp. 170-183, 2017.
[19] L.A. Kloiber, D.E. Eckmann, T.R. Meyer, and S.J. Hautzinger, "Design considerations in cable-stayed roof structures," *Modern Steel Construction*, vol. *44*, no. 3, pp. 75-84, 2004.
[20] H.A. Buchholdt, "Cable beams and cable grids," in *An introduction to cable roof structures*, 2nd ed., London: Thomas Telford, 1999, pp. 182-230.
[21] Standard Specification for Zinc-Coated Parallel and Helical Steel Wire Structural Strand, A586 − 04a, 2009.